Electronic Supplementary Material (ESI) for Dalton Transactions.


# Chemical Bonding in Actinyl (V/VI) Dipyriamethyrin Complexes for the Actinide Series from Americium to Californium: A Computational Investigation

Abigail Jennifer G[1], Yang Gao[2,3,4], Georg Schreckenbach[2]* and Elumalai Varathan[1]*

[1]Department of Chemistry, SRM Institute of Science and Technology, Kattankulathur, Chennai 603203, Tamil Nadu, India.
[2]Department of Chemistry, University of Manitoba, Winnipeg, Manitoba, R3T 2N2, Canada.
[3]Institut National de La Recherche Scientifique (INRS)-Centre Énergie Matériaux Télécommunications, Varennes, QC, J3X 1P7, Canada.
[4]Institute of Fundamental and Frontier Sciences, University of Electronic Science and Technology of China, Chengdu, Sichuan 610054, China.

Email: schrecke@cc.umanitoba.ca
varathan.elumalai85@gmail.com, varathae@srmist.edu.in

## CONTENT CAPTIONS

**Table S1. Bond parameters computed at PBE/ZORA-TZP level of theory (gas phase). Bond lengths (Å), bond angles (°), bond orders (B.O), charges, spin densities on the actinide and $O_{yl}$ atoms (a.u.), and actinyl stretching vibrational frequencies ($cm^{-1}$) of the bare actinyl (V,VI) cations.**

| | An=$O_{yl}$ | O=An=O | B.O. | Mayer B.O. | Q(An) | Q(O1/O2) | Spin on An | Spin on $O_{yl}$ | $\nu_{symm}$ ($AnO_2$-L) | $\nu_{asymm}$ ($AnO_2$-L) |
|---|---|---|---|---|---|---|---|---|---|---|
| $Am^{V}O_2^{+}$ | 1.745 | 180.0 | 2.059 | 2.105 | 1.648 | -0.324 | 4.518 | -0.259 | 845.0 | 963.1 |
| $Cm^{V}O_2^{+}$ | 1.767 | 180.0 | 1.718 | 2.005 | 1.816 | -0.408 | 5.198 | -0.099 | 808.8 | 907.6 |
| $Bk^{V}O_2^{+}$ | 1.775 | 180.0 | 1.674 | 1.930 | 1.972 | -0.486 | 5.343 | 0.329 | 826.0 | 909.1 |
| $Cf^{V}O_2^{+}$ | 1.866 | 94.9 | 1.949 | 2.036 | 1.867 | -0.433 | 4.966 | 1.017 | 696.8 | 598.7 |
| $Am^{VI}O_2^{2+}$ | 1.698 | 180.0 | 2.210 | 2.198 | 2.242 | -0.121 | 3.452 | -0.226 | 915.3 | 1053.0 |
| $Cm^{VI}O_2^{2+}$ | 1.712 | 180.0 | 2.077 | 2.102 | 1.983 | 0.008 | 4.719 | -0.359 | 830.2 | 986.6 |
| $Bk^{VI}O_2^{2+}$ | 1.744 | 179.9 | 1.818 | 1.952 | 2.161 | -0.080 | 5.033 | -0.016 | 795.0 | 903.5 |
| $Cf^{VI}O_2^{2+}$ | 1.795 | 158.4 | 1.758 | 1.936 | 2.245 | -0.123 | 4.565 | 0.717 | 697.1 | 706.5 |

**Table S2. Bond parameters (i.e., bond lengths (Å) and bond angles (°)) computed at the PBE/TZP level of theory in the gas phase for the actinyl (V and VI) complexes**

| | An-N1 | An-N2 | An-N3 | An-N4 | An-N5 | An-N6 | $An=O_{yl}(1)$ | $An=O_{yl}(2)$ |
|---|---|---|---|---|---|---|---|---|
| | | | | Bond Lengths | | | | |
| $Am^{V}O2\text{-}L^{-}$ | 2.897 | 2.801 | 2.808 | 2.897 | 2.801 | 2.808 | 1.798 | 1.799 |
| $Cm^{V}O2\text{-}L^{-}$ | 2.872 | 2.785 | 2.808 | 2.892 | 2.800 | 2.801 | 1.821 | 1.824 |
| $Bk^{V}O2\text{-}L^{-}$ | 2.864 | 2.779 | 2.783 | 2.861 | 2.767 | 2.774 | 1.828 | 1.831 |
| $Cf^{V}O2\text{-}L^{-}$ | 2.802 | 2.691 | 2.698 | 2.831 | 2.780 | 2.802 | 1.817 | 1.820 |
| $Am^{VI}O2\text{-}L$ | 2.758 | 2.656 | 2.658 | 2.758 | 2.656 | 2.658 | 1.761 | 1.763 |
| $Cm^{VI}O2\text{-}L$ | 2.798 | 2.764 | 2.786 | 2.816 | 2.695 | 2.692 | 1.778 | 1.783 |
| $Bk^{VI}O2\text{-}L$ | 2.817 | 2.741 | 2.739 | 2.811 | 2.727 | 2.740 | 1.814 | 1.816 |
| $Cf^{VI}O2\text{-}L$ | 2.811 | 2.723 | 2.733 | 2.811 | 2.731 | 2.740 | 1.812 | 1.815 |
| | | | | Bond Angles | | | | |
| | $O_{yl}=An=O_{yl}$ | N1-An-N2 | N2-An-N3 | N3-An-N4 | N4-An-N5 | N5-An-N6 | N6-An-N1 | |
| $Am^{V}O2\text{-}L^{-}$ | 180.0 | 57.9 | 65.9 | 57.6 | 57.9 | 65.9 | 57.6 | |
| $Cm^{V}O2\text{-}L^{-}$ | 179.9 | 58.3 | 65.7 | 57.6 | 57.9 | 65.6 | 57.8 | |
| $Bk^{V}O2\text{-}L^{-}$ | 180.0 | 58.1 | 65.5 | 57.9 | 58.3 | 65.8 | 58.0 | |
| $Cf^{V}O2\text{-}L^{-}$ | 179.5 | 59.1 | 66.4 | 58.8 | 57.8 | 64.5 | 58.4 | |
| $Am^{VI}O2\text{-}L$ | 180.0 | 59.2 | 65.6 | 59.0 | 59.2 | 65.6 | 59.0 | |
| $Cm^{VI}O2\text{-}L$ | 179.9 | 58.7 | 64.1 | 58.0 | 59.0 | 66.5 | 58.8 | |
| $Bk^{VI}O2\text{-}L$ | 179.9 | 58.5 | 65.3 | 58.3 | 58.7 | 65.5 | 58.2 | |
| $Cf^{VI}O2\text{-}L$ | 180.0 | 58.8 | 65.5 | 58.2 | 58.7 | 65.3 | 58.1 | |

**Table S3. Calculated bond lengths (Å) and bond angles (deg) of the actinyl (VI and V) complexes at the PBE/TZP level of theory using ADF and ZORA in $CH_2Cl_2$ solvent**

| | An-N1 | An-N2 | An-N3 | An-N4 | An-N5 | An-N6 | $An=O_{yl}(1)$ | $An=O_{yl}(2)$ |
|---|---|---|---|---|---|---|---|---|
| | | | | Bond Lengths | | | | |
| $Am^{V}O_2$-$L^-$ | 2.883 | 2.777 | 2.782 | 2.883 | 2.777 | 2.782 | 1.817 | 1.818 |
| $Cm^{V}O_2$-$L^-$ | 2.859 | 2.758 | 2.772 | 2.874 | 2.769 | 2.767 | 1.838 | 1.838 |
| $Bk^{V}O_2$-$L^-$ | 2.837 | 2.745 | 2.747 | 2.836 | 2.736 | 2.741 | 1.843 | 1.845 |
| $Cf^{V}O_2$-$L^-$ | 2.795 | 2.686 | 2.699 | 2.814 | 2.789 | 2.778 | 1.838 | 1.839 |
| $Am^{VI}O_2$-L | 2.897 | 2.800 | 2.808 | 2.897 | 2.800 | 2.808 | 1.798 | 1.799 |
| $Cm^{VI}O_2$-L | 2.825 | 2.758 | 2.768 | 2.834 | 2.734 | 2.733 | 1.815 | 1.814 |
| $Bk^{VI}O_2$-L | 2.818 | 2.743 | 2.743 | 2.810 | 2.735 | 2.742 | 1.841 | 1.840 |
| $Cf^{VI}O_2$-L | 2.817 | 2.734 | 2.739 | 2.818 | 2.739 | 2.745 | 1.832 | 1.830 |
| | | | | Bond Angles | | | | |
| | $O_{yl}=An=O_{yl}$ | N1-An-N2 | N2-An-N3 | N3-An-N4 | N4-An-N5 | N5-An-N6 | N6-An-N1 | |
| $Am^{V}O_2$-$L^-$ | 180.0 | 58.0 | 65.8 | 88.6 | 58.0 | 65.8 | 57.7 | |
| $Cm^{V}O_2$-$L^-$ | 180.0 | 58.3 | 65.7 | 57.8 | 58.0 | 65.6 | 58.0 | |
| $Bk^{V}O_2$-$L^-$ | 180.0 | 58.4 | 65.4 | 58.2 | 58.5 | 65.6 | 58.2 | |
| $Cf^{V}O_2$-$L^-$ | 179.7 | 59.2 | 65.9 | 58.8 | 58.2 | 64.2 | 58.4 | |
| $Am^{VI}O_2$-L | 180.0 | 57.9 | 65.9 | 57.6 | 57.9 | 65.9 | 57.6 | |
| $Cm^{VI}O_2$-L | 179.9 | 58.4 | 65.0 | 57.9 | 58.5 | 65.8 | 58.3 | |
| $Bk^{VI}O_2$-L | 179.9 | 58.5 | 65.2 | 58.3 | 58.7 | 65.3 | 58.3 | |

| | | | | | | | |
|---|---|---|---|---|---|---|---|
| $Cf^{VI}O_2$-L | 180.0 | 58.6 | 65.4 | 58.2 | 58.5 | 65.3 | 58.1 |

**Table S4. Mayer, Nalewajski-Mrozek and Gophinatan-Jug Bond Orders of the Actinyl (V and VI) Complexes**

| | $Am^{V}O_2$-$L^-$ | $Cm^{V}O_2$-$L^-$ | $Bk^{V}O_2$-$L^-$ | $Cf^{V}O_2$-$L^-$ | $Am^{VI}O_2$-L | $Cm^{VI}O_2$-L | $Bk^{VI}O_2$-L | $Cf^{VI}O_2$-L |
|---|---|---|---|---|---|---|---|---|
| Mayer Bond Orders | | | | | | | | |
| $An{=}O_{yl}(1)$ | 1.843 | 1.732 | 1.679 | 1.652 | 1.862 | 1.717 | 1.642 | 1.664 |
| $An{=}O_{yl}(2)$ | 1.860 | 1.753 | 1.693 | 1.670 | 1.887 | 1.743 | 1.656 | 1.682 |
| An-N1 | 0.121 | 0.116 | 0.126 | 0.137 | 0.218 | 0.157 | 0.145 | 0.135 |
| An-N2 | 0.167 | 0.165 | 0.173 | 0.166 | 0.287 | 0.228 | 0.194 | 0.184 |
| An-N3 | 0.165 | 0.164 | 0.171 | 0.173 | 0.287 | 0.228 | 0.191 | 0.180 |
| An-N4 | 0.121 | 0.120 | 0.125 | 0.148 | 0.218 | 0.161 | 0.144 | 0.134 |
| An-N5 | 0.168 | 0.168 | 0.170 | 0.203 | 0.287 | 0.199 | 0.190 | 0.185 |
| An-N6 | 0.165 | 0.163 | 0.169 | 0.205 | 0.287 | 0.204 | 0.192 | 0.182 |
| Nalewajski-Mrozek Bond Orders | | | | | | | | |
| $An{=}O_{yl}(1)$ | 2.006 | 2.315 | 1.813 | 1.769 | 1.994 | 2.297 | 1.737 | 1.765 |
| $An{=}O_{yl}(2)$ | 2.015 | 2.330 | 1.824 | 1.783 | 2.004 | 2.321 | 1.747 | 1.779 |
| An-N1 | 0.112 | 0.223 | 0.131 | 0.153 | 0.208 | 0.262 | 0.146 | 0.151 |
| An-N2 | 0.157 | 0.293 | 0.181 | 0.182 | 0.280 | 0.360 | 0.195 | 0.206 |
| An-N3 | 0.156 | 0.294 | 0.180 | 0.193 | 0.282 | 0.362 | 0.193 | 0.204 |
| An-N4 | 0.112 | 0.230 | 0.130 | 0.166 | 0.208 | 0.193 | 0.143 | 0.150 |
| An-N5 | 0.157 | 0.299 | 0.178 | 0.226 | 0.280 | 0.316 | 0.191 | 0.208 |
| An-N6 | 0.156 | 0.291 | 0.178 | 0.231 | 0.282 | 0.323 | 0.193 | 0.206 |
| Gophinatan-Jug Bond Order | | | | | | | | |
| $An{=}O_{yl}(1)$ | 1.593 | 2.100 | 1.271 | 1.268 | 1.648 | 2.178 | 1.274 | 1.275 |
| $An{=}O_{yl}(2)$ | 1.602 | 2.114 | 1.280 | 1.279 | 1.658 | 2.156 | 1.282 | 1.287 |
| An-N1 | 0.096 | 0.207 | 0.100 | 0.117 | 0.181 | 0.248 | 0.114 | 0.115 |
| An-N2 | 0.135 | 0.273 | 0.137 | 0.138 | 0.244 | 0.343 | 0.152 | 0.157 |
| An-N3 | 0.134 | 0.274 | 0.138 | 0.147 | 0.245 | 0.346 | 0.151 | 0.155 |

| | | | | | | | | |
|---|---|---|---|---|---|---|---|---|
| An-N4 | 0.096 | 0.214 | 0.099 | 0.127 | 0.181 | 0.151 | 0.112 | 0.115 |
| An-N5 | 0.135 | 0.278 | 0.135 | 0.172 | 0.244 | 0.300 | 0.149 | 0.159 |
| An-N6 | 0.134 | 0.271 | 0.135 | 0.176 | 0.245 | 0.307 | 0.151 | 0.157 |

**Table S5. Calculated nitrogen NPA charges on the free actinyl (V and VI) cations and ligand anion at the PBE/TZP level of theory in gas phase**

| | $Am^{V}O_2^{+}$ | $Cm^{V}O_2^{+}$ | $Bk^{V}O_2^{+}$ | $Cf^{V}O_2^{+}$ | $Am^{VI}O_2^{2+}$ | $Cm^{VI}O_2^{2+}$ | $Bk^{VI}O_2^{2+}$ | $Cf^{VI}O_2^{2+}$ |
|---|---|---|---|---|---|---|---|---|
| Q(An) | 1.648 | 1.816 | 1.972 | 1.867 | 2.242 | 1.983 | 2.161 | 2.245 |
| $Q(O_{yl}(1/2))$ | -0.323 | -0.408 | -0.486 | -0.433 | -0.121 | 0.008 | -0.080 | -0.123 |
| **Free ligand anion** | | | | | | | | |
| N1/N4 | -0.342 | | | | | | | |
| N2/N5 | -0.352 | | | | | | | |
| N3/N6 | -0.356 | | | | | | | |

**Table S6. NPA charges on the actinide and donor atoms (atomic units) of the actinyl (V and VI) complexes using the PBE/ZORA-TZP level of theory in gas phase**

| | $Am^{V}O_2$-$L^-$ | $Cm^{V}O_2$-$L^-$ | $Bk^{V}O_2$-$L^-$ | $Cf^{V}O_2$-$L^-$ | $Am^{VI}O_2$-L | $Cm^{VI}O_2$-L | $Bk^{VI}O_2$-L | $Cf^{VI}O_2$-L |
|---|---|---|---|---|---|---|---|---|
| (An) | 1.237 | 1.398 | 1.516 | 1.431 | 1.216 | 1.302 | 1.470 | 1.417 |
| ($O_{yl}$(1)) | -0.422 | -0.515 | -0.593 | -0.516 | -0.311 | -0.316 | -0.494 | -0.497 |
| ($O_{yl}$(2)) | -0.416 | -0.506 | -0.584 | -0.506 | -0.303 | -0.300 | -0.483 | -0.485 |
| (N1) | -0.385 | -0.384 | -0.383 | -0.391 | -0.363 | -0.393 | -0.384 | -0.378 |
| (N2) | -0.421 | -0.423 | -0.421 | -0.414 | -0.401 | -0.439 | -0.432 | -0.423 |
| (N3) | -0.419 | -0.421 | -0.419 | -0.414 | -0.400 | -0.437 | -0.430 | -0.422 |
| (N4) | -0.385 | -0.385 | -0.382 | -0.393 | -0.363 | -0.394 | -0.384 | -0.378 |
| (N5) | -0.421 | -0.424 | -0.420 | -0.462 | -0.401 | -0.434 | -0.430 | -0.424 |
| (N6) | -0.419 | -0.421 | -0.419 | -0.460 | -0.400 | -0.432 | -0.431 | -0.423 |

**Table S7. Natural Orbital Populations and spin density of An (An = Am, Cm, Bk and Cf) centers in actinyl (VI and V) complexes**

| Complex | Natural Orbital Population | | | | Spin Density on An | | |
|---|---|---|---|---|---|---|---|
| | 5f | 6d | 7s | 7p | Complex[a] | Bare actinyl[b] | An[c] |
| $Am^{V}O_2$-$L^-$ | 6.38 | 1.14 | 0.17 | 0.01 | 4.459 | 4.518 | $f^4$ |
| $Cm^{V}O_2$-$L^-$ | 7.20 | 1.17 | 0.17 | 0.01 | 5.269 | 5.198 | $f^5$ |
| $Bk^{V}O_2$-$L^-$ | 8.00 | 1.25 | 0.18 | 0.01 | 5.478 | 5.343 | $f^6$ |
| $Cf^{V}O_2$-$L^-$ | 9.10 | 1.23 | 0.18 | 0.01 | 4.388 | 4.966 | $f^7$ |
| $Am^{VI}O_2$-L | 6.33 | 1.38 | 0.19 | 0.01 | 3.680 | 3.452 | $f^3$ |
| $Cm^{VI}O_2$-L | 7.18 | 1.27 | 0.19 | 0.01 | 4.892 | 4.719 | $f^4$ |
| $Bk^{VI}O_2$-L | 7.99 | 1.30 | 0.18 | 0.01 | 5.350 | 5.033 | $f^5$ |
| $Cf^{VI}O_2$-L | 9.10 | 1.25 | 0.18 | 0.01 | 4.395 | 4.565 | $f^6$ |

[a]Actinide spin densities for actinyl (V and VI) complexes. [b]Actinide spin densities for bare actinyl (V and VI) cations, calculated at the same level of theory. [c]Formal f-orbital occupations corresponding to formal actinide spin densities for the actinyl (V and VI) cations.

**Table S8. Natural Orbital Population and spin density of An (An = Am, Cm, Bk and Cf) centers in the bare actinyl (V and VI) cations**

| Actinyl | NPA Charge | Natural Orbital Population | | | | Spin Density |
|---|---|---|---|---|---|---|
| Moiety | An | 5f | 6d | 7s | 7p | An |
| $Am^{V}O_2^{+}$ | -0.324 | 6.53 | 0.80 | 0.03 | 0.00 | 4.518 |
| $Cm^{V}O_2^{+}$ | -0.408 | 7.36 | 0.81 | 0.03 | 0.00 | 5.198 |
| $Bk^{V}O_2^{+}$ | -0.486 | 8.17 | 0.85 | 0.03 | 0.01 | 5.343 |
| $Cf^{V}O_2^{+}$ | -0.433 | 9.21 | 0.84 | 0.01 | 0.08 | 4.966 |
| $Am^{VI}O_2^{2+}$ | -0.121 | 6.12 | 0.87 | 0.03 | 0.00 | 3.452 |
| $Cm^{VI}O_2^{2+}$ | 0.008 | 7.22 | 0.80 | 0.02 | 0.00 | 4.719 |
| $Bk^{VI}O_2^{2+}$ | -0.080 | 8.04 | 0.81 | 0.02 | 0.00 | 5.033 |
| $Cf^{VI}O_2^{2+}$ | -0.123 | 9.05 | 0.71 | 0.02 | 0.00 | 4.565 |

**Table S9. Calculated spin density on the actinide and donor atoms (atomic units) of the actinyl (V and VI) complexes at the PBE/ZORA-TZP level of theory in gas phase**

| | $Am^{V}O_2$-$L^-$ | $Cm^{V}O_2$-$L^-$ | $Bk^{V}O_2$-$L^-$ | $Cf^{V}O_2$-$L^-$ | $Am^{VI}O_2$-L | $Cm^{VI}O_2$-L | $Bk^{VI}O_2$-L | $Cf^{VI}O_2$-L |
|---|---|---|---|---|---|---|---|---|
| An | 4.459 | 5.269 | 5.478 | 4.388 | 3.680 | 4.892 | 5.350 | 4.395 |
| An[a] | V | V | VI | V | VI | VI | VI | V |
| $O_{yl}$(1) | -0.266 | -0.155 | 0.218 | 0.315 | -0.217 | -0.241 | 0.141 | 0.322 |
| $O_{yl}$(2) | -0.267 | -0.160 | 0.216 | 0.316 | -0.219 | -0.250 | 0.134 | 0.325 |
| (N1) | 0.004 | 0.007 | 0.009 | 0.090 | -0.033 | 0.007 | 0.011 | 0.023 |
| (N2) | 0.003 | 0.005 | 0.015 | 0.020 | -0.032 | 0.015 | 0.035 | 0.014 |
| (N3) | 0.003 | 0.005 | 0.015 | 0.024 | -0.033 | 0.016 | 0.034 | 0.011 |
| (N4) | 0.004 | 0.007 | 0.009 | 0.094 | -0.033 | 0.008 | 0.010 | 0.023 |
| (N5) | 0.003 | 0.005 | 0.015 | 0.089 | -0.032 | 0.015 | 0.032 | 0.015 |
| (N6) | 0.003 | 0.005 | 0.015 | 0.089 | -0.032 | 0.016 | 0.037 | 0.011 |

[a]Assigned oxidation states of the actinide based on the gas-phase optimized geometries and spin density

**Table S10. Natural electron configurations of the actinide in the free actinyl (VI and V) cations**

| Actinyl moiety | alpha | | | | beta | | | |
|---|---|---|---|---|---|---|---|---|
| | 5f | 6d | 7s | 7p | 5f | 6d | 7s | 7p |
| $Am^{V}O_2^{+}$ | 5.49 | 0.43 | 0.02 | 0.00 | 1.04 | 0.36 | 0.02 | 0.00 |
| $Cm^{V}O_2^{+}$ | 6.25 | 0.43 | 0.02 | 0.00 | 1.11 | 0.37 | 0.01 | 0.00 |
| $Bk^{V}O_2^{+}$ | 6.75 | 0.43 | 0.01 | 0.00 | 1.42 | 0.42 | 0.01 | 0.00 |
| $Cf^{V}O_2^{+}$ | 6.96 | 0.52 | 0.06 | 0.01 | 2.24 | 0.32 | 0.02 | 0.00 |
| $Am^{VI}O_2^{2+}$ | 4.76 | 0.46 | 0.02 | 0.00 | 1.36 | 0.41 | 0.01 | 0.00 |
| $Cm^{VI}O_2^{2+}$ | 5.93 | 0.44 | 0.01 | 0.00 | 1.29 | 0.36 | 0.01 | 0.00 |
| $Bk^{VI}O_2^{2+}$ | 6.51 | 0.43 | 0.01 | 0.00 | 1.53 | 0.38 | 0.01 | 0.00 |
| $Cf^{VI}O_2^{2+}$ | 6.78 | 0.38 | 0.01 | 0.00 | 2.26 | 0.34 | 0.01 | 0.00 |

**Table S11. Natural electron configurations of the actinide in actinyl (VI and V) complexes**

| Complex | alpha | | | | beta | | | |
|---|---|---|---|---|---|---|---|---|
| | 5f | 6d | 7s | 7p | 5f | 6d | 7s | 7p |
| $Am^{V}O_2$-$L^{-}$ | 5.38 | 0.61 | 0.09 | 0.00 | 1.00 | 0.53 | 0.08 | 0.01 |
| $Cm^{V}O_2$-$L^{-}$ | 6.19 | 0.62 | 0.09 | 0.00 | 1.01 | 0.55 | 0.08 | 0.01 |
| $Bk^{V}O_2$-$L^{-}$ | 6.72 | 0.64 | 0.09 | 0.00 | 1.65 | 0.61 | 0.08 | 0.00 |

| | | | | | | | | |
|---|---|---|---|---|---|---|---|---|
| $Cf^{V}O_2$-L$^-$ | 6.74 | 0.62 | 0.09 | 0.00 | 2.36 | 0.62 | 0.09 | 0.00 |
| $Am^{VI}O_2$-L | 4.96 | 0.73 | 0.10 | 0.01 | 1.37 | 0.65 | 0.09 | 0.01 |
| $Cm^{VI}O_2$-L | 5.99 | 0.68 | 0.10 | 0.00 | 1.19 | 0.59 | 0.09 | 0.00 |
| $Bk^{VI}O_2$-L | 6.65 | 0.67 | 0.09 | 0.01 | 1.35 | 0.63 | 0.09 | 0.00 |
| $Cf^{VI}O_2$-L | 6.74 | 0.62 | 0.09 | 0.01 | 2.36 | 0.62 | 0.09 | 0.00 |

**Table S12. QTAIM analysis of electron density ($\rho_C$) at An-N and An=$O_{yl}$ bond critical points (e/bohr$^3$) computed at the ZORA/PBE level of theory in gas phase.**

| Complex | An-N1 | An-N2 | An-N3 | An-N4 | An-N5 | An-N6 | An=$O_{yl}$(1) | An=$O_{yl}$(2) | N2-N3 | N5-N6 |
|---|---|---|---|---|---|---|---|---|---|---|
| $Am^{V}O_2$-L$^-$ | 0.0238 | 0.0298 | 0.0294 | 0.0238 | 0.0298 | 0.0294 | 0.272 | 0.271 | - | - |
| $Cm^{V}O_2$-L$^-$ | 0.0234 | 0.0291 | 0.0291 | 0.0244 | 0.0300 | 0.0287 | 0.254 | 0.253 | 0.0093 | 0.0094 |
| $Bk^{V}O_2$-L$^-$ | 0.0239 | 0.0293 | 0.0291 | 0.0240 | 0.0301 | 0.0297 | 0.246 | 0.246 | 0.0096 | 0.0096 |
| $Cf^{V}O_2$-L$^-$ | 0.0266 | 0.0345 | 0.0341 | 0.0250 | 0.0268 | 0.0283 | 0.246 | 0.245 | 0.0109 | 0.0100 |
| $Am^{VI}O_2$-L | 0.0323 | 0.0406 | 0.0406 | 0.0323 | 0.0406 | 0.0406 | 0.295 | 0.294 | - | - |
| $Cm^{VI}O_2$-L | 0.0286 | 0.0311 | 0.0298 | 0.0275 | 0.0364 | 0.0366 | 0.281 | 0.277 | 0.0109 | - |
| $Bk^{VI}O_2$-L | 0.0268 | 0.0327 | 0.0318 | 0.0265 | 0.0317 | 0.0319 | 0.254 | 0.252 | 0.0107 | 0.0106 |
| $Cf^{VI}O_2$-L | 0.0260 | 0.0313 | 0.0308 | 0.0259 | 0.0318 | 0.0313 | 0.250 | 0.247 | 0.0106 | 0.0106 |

**Table S13. Calculated bond lengths (Å) and bond angles (°) of the actinyl (V and VI) dichloride at the PBE/ZORA-TZP level of theory in $CH_2Cl_2$ medium.**

| | $Am^{V}O_2Cl_2^-$ | $Cm^{V}O_2Cl_2^-$ | $Bk^{V}O_2Cl_2^-$ | $Cf^{V}O_2Cl_2^-$ | $Am^{VI}O_2Cl_2$ | $Cm^{VI}O_2Cl_2$ | $Bk^{VI}O_2Cl_2$ | $Cf^{VI}O_2Cl_2$ |
|---|---|---|---|---|---|---|---|---|
| Bond Length | | | | | | | | |
| An=O | 1.803 | 1.825 | 1.835 | 1.928 | 1.751 | 1.756 | 1.790 | 1.890 |
| An-Cl | 2.720 | 2.683 | 2.634 | 2.610 | 2.592 | 2.585 | 2.580 | 2.492 |
| Bond Angle | | | | | | | | |
| O=An=O | 178.8 | 177.1 | 170.8 | 105.9 | 179.9 | 177.5 | 180.0 | 92.9 |
| Cl-An-Cl | 107.2 | 108.6 | 98.6 | 107.2 | 177.4 | 104.0 | 161.3 | 90.4 |

**Table S14. Calculated formation energy (ΔE) for the complexation reaction (eq. 1 and eq. 2) with scalar relativity and with SOC relativity (kcal/mol)**

| | $Am^{V}O_2$-$L^-$ | $Cm^{V}O_2$-$L^-$ | $Bk^{V}O_2$-$L^-$ | $Cf^{V}O_2$-$L^-$ | $Am^{VI}O_2$-L | $Cm^{VI}O_2$-L | $Bk^{VI}O_2$-L | $Cf^{VI}O_2$-L |
|---|---|---|---|---|---|---|---|---|
| Eq. 1– ΔE - SCALAR | -294.1 | -302.8 | -312.8 | -304.8 | -619.1 | -595.9 | -619.0 | -641.0 |
| Eq. 1 – ΔE - SOC | -318.6 | -332.2 | -335.2 | -364.7 | -615.4 | -601.2 | -614.5 | -628.3 |
| Eq. 2 – ΔE - SCALAR | 32.7 | 31.6 | 31.0 | 44.5 | 19.1 | 5.7 | 66.8 | -98.9 |
| Eq. 2 – ΔE - SOC | 12.6 | -5.1 | -12.7 | 27.8 | 1.4 | -14.3 | -26.01 | -51.2 |

**Table S15. EDA results (kcal/mol) for the actinyl (V and VI) complexes in the gas phase at the PBE/TZP level of theory**

| Energy Terms | Interacting Fragments | | | |
|---|---|---|---|---|
| | $L^{2-}$ vs. $Am^{V}O_2^{+}$ | $L^{2-}$ vs. $Cm^{V}O_2^{+}$ | $L^{2-}$ vs. $Bk^{V}O_2^{+}$ | $L^{2-}$ vs. $Cf^{V}O_2^{+}$ |
| $\Delta E_{int}$ | -305.35 | -313.75 | -326.64 | -384.39 |
| $\Delta E_{steric}$ | -211.68 | -214.95 | -220.42 | -223.22 |
| $\Delta E_{Pauli}$ | 72.87 (23.86%) | 74.76 (23.83%) | 76.20 (23.32%) | 83.18 (21.64%) |
| $\Delta E_{el\text{-}static}$ | -284.55 (93.19%) | -289.70 (92.33%) | -296.62 (90.81%) | -306.40 (79.71%) |
| $\Delta E_{orb}$ | -93.67 (30.68%) | -98.81 (31.49%) | -106.22 (32.52%) | -161.17 (41.93%) |
| Energy Terms | Interacting Fragments | | | |
| | $L^{2-}$ vs. $Am^{VI}O_2^{2+}$ | $L^{2-}$ vs. $Cm^{VI}O_2^{2+}$ | $L^{2-}$ vs. $Bk^{VI}O_2^{2+}$ | $L^{2-}$ vs. $Cf^{VI}O_2^{2+}$ |
| $\Delta E_{int}$ | -584.37 | -617.03 | -638.41 | -660.43 |
| $\Delta E_{steric}$ | -391.01 | -392.70 | -396.97 | -399.55 |
| $\Delta E_{Pauli}$ | 117.87 (20.17%) | 90.71 (14.70%) | 86.56 (13.56%) | 85.31 (12.92%) |
| $\Delta E_{el\text{-}static}$ | -508.89 (87.08%) | -483.41 (78.34%) | -483.53 (75.74%) | -484.86 (73.42%) |
| $\Delta E_{orb}$ | -193.35 (33.09%) | -224.33 (36.36%) | -241.44 (37.82%) | -260.87 (39.50%) |

**Table S16. Selected NOCVs with Energy Values $\Delta E_i^{orb}$ ($i$ = 1–10) and NOCV Contour Plots of the Deformation Density[a]**

| *i* | Orbital Type | Complex | $\Delta E_i^{orb}$ (kcal/mol) | | | | Dominant NOCV |
|---|---|---|---|---|---|---|---|
| | | | Am | Cm | Bk | Cf | |
| 1 | σ | $[AnO_2L]^{-1}$ | -8.150 | -10.411 | -14.551 | -28.599 | 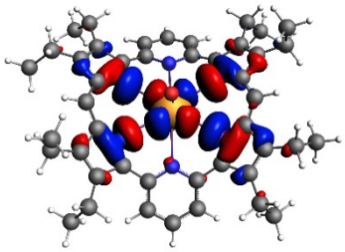 |
| | | $[AnO_2L]^{0}$ | 21.410 | -45.940 | -70.841 | -74.415 | |
| 2 | σ | $[AnO_2L]^{-1}$ | -13.701 | -12.543 | -15.802 | -26.943 | 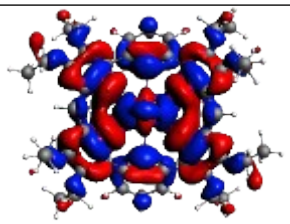 |
| | | $[AnO_2L]^{0}$ | -43.985 | -18.785 | -24.658 | -32.495 | |
| 3 | σ | $[AnO_2L]^{-1}$ | -6.476 | -13.574 | -14.136 | -15.075 | 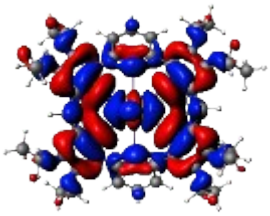 |
| | | $[AnO_2L]^{0}$ | - | -22.932 | -15.593 | -16.902 | |
| 4 | σ | $[AnO_2L]^{-1}$ | -11.947 | -11.831 | -8.134 | -12.733 | 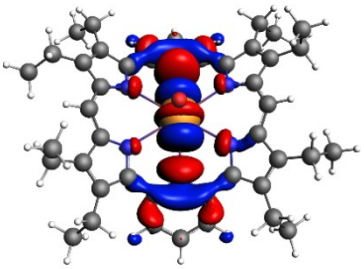 |
| | | $[AnO_2L]^{0}$ | -16.831 | -20.772 | -20.472 | -9.792 | |
| 5 | σ | $[AnO_2L]^{-1}$ | -8.723 | -4.645 | -5.128 | -7.504 | 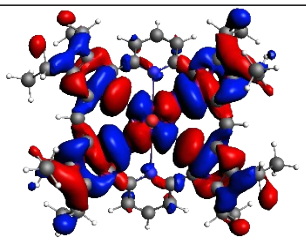 |
| | | $[AnO_2L]^{0}$ | -12.956 | -16.890 | -14.575 | -14.277 | |
| 6 | σ | $[AnO_2L]^{-1}$ | -4.862 | -3.766 | -4.603 | -10.274 | 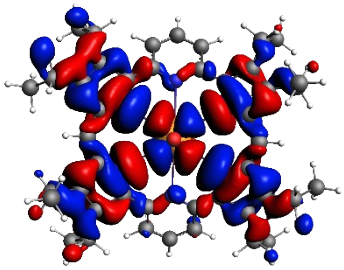 |
| | | $[AnO_2L]^{0}$ | -23.006 | -9.084 | -6.590 | -8.794 | |

| | | | | | | | |
|---|---|---|---|---|---|---|---|
| 7 | σ | $[AnO_2L]^{-1}$ | -4.249 | -3.725 | -4.127 | -9.595 | 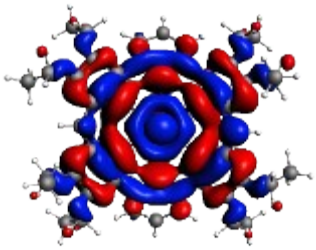 |
| | | $[AnO_2L]^{0}$ | -19.130 | -8.552 | -7.757 | -11.571 | |
| 8 | σ | $[AnO_2L]^{-1}$ | -3.372 | -3.332 | -3.249 | -8.425 | 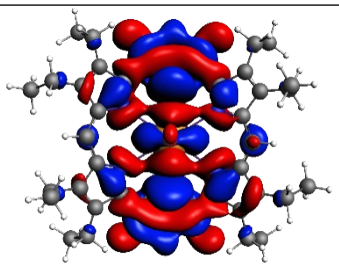 |
| | | $[AnO_2L]^{0}$ | -12.190 | -7.844 | -7.129 | -9.605 | |
| 9 | π | $[AnO_2L]^{-1}$ | -2.906 | -2.772 | -3.579 | -3.362 | 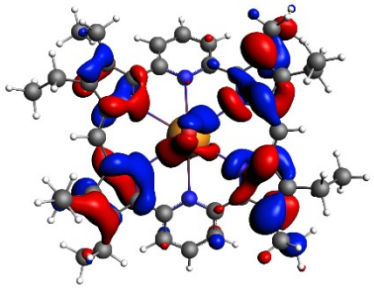 |
| | | $[AnO_2L]^{0}$ | -3.799 | -6.727 | -3.287 | -4.704 | |
| 10 | π | $[AnO_2L]^{-1}$ | -2.313 | -2.835 | -2.703 | -3.396 | 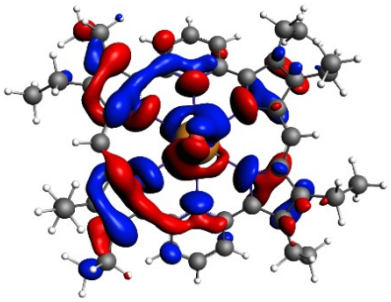 |
| | | $[AnO_2L]^{0}$ | -5.504 | -4.264 | -4.703 | -3.806 | |
| [a]Blue – Density inflow; Red – Density outflow (isosurface value: 0.01) | | | | | | | |

| COMPLEX | TOP VIEW | SIDE VIEW |
|---|---|---|
| $Am^{V}O_2$-$L^-$ | 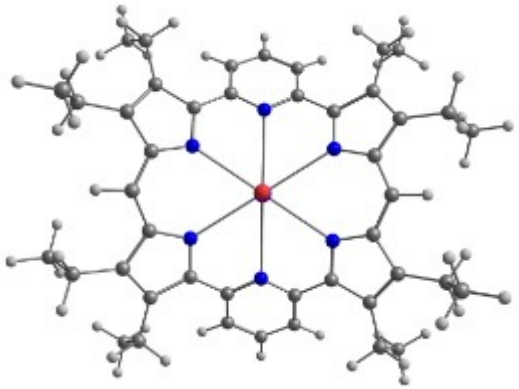 | 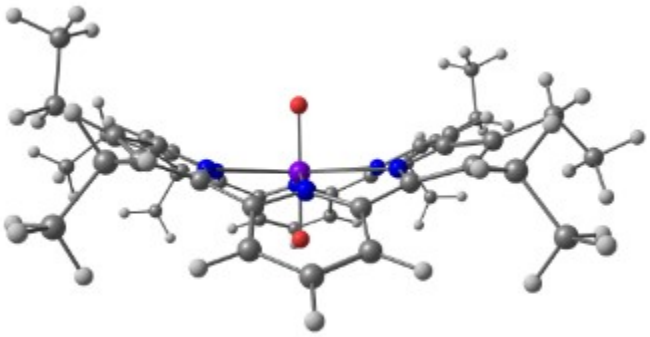 |
| $Cm^{V}O_2$-$L^-$ | 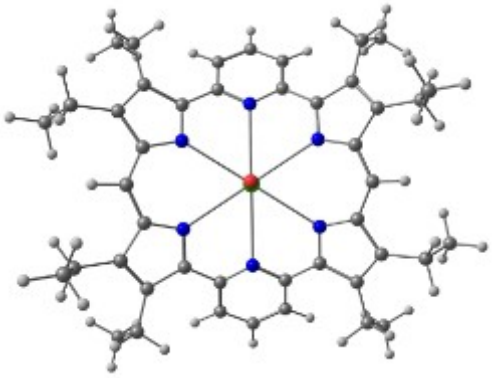 | 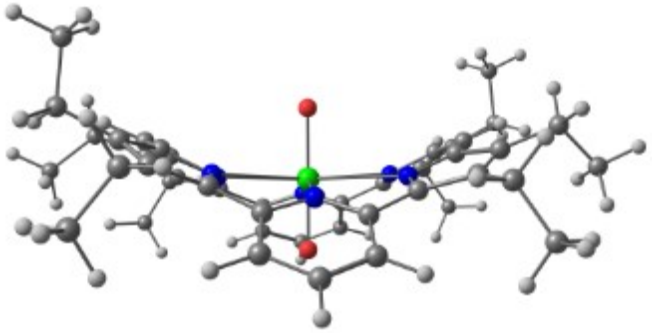 |
| $Bk^{V}O_2$-$L^-$ | 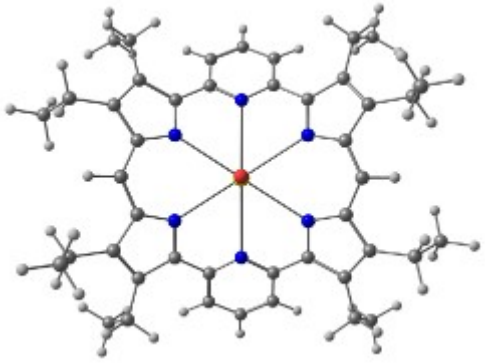 | 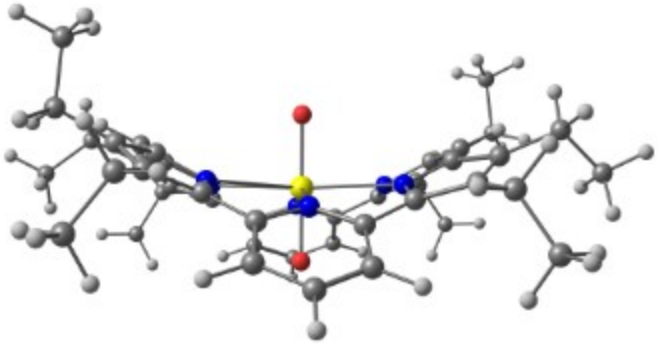 |
| $Cf^{V}O_2$-$L^-$ | 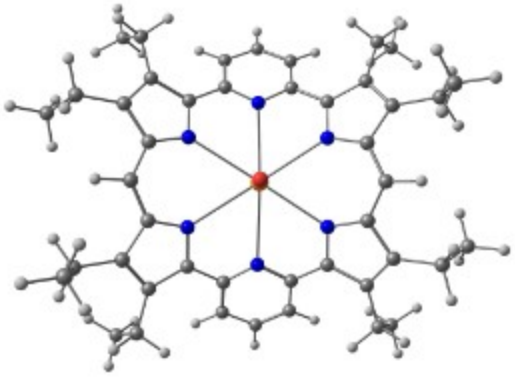 | 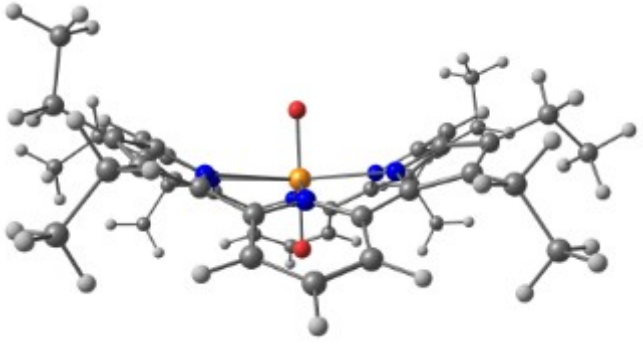 |

| | | |
|---|---|---|
| $Am^{VI}O_2$-$L^-$ | 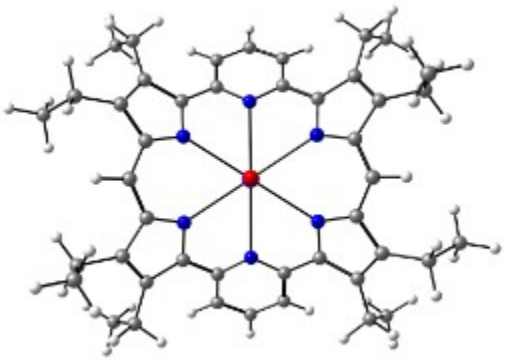 | 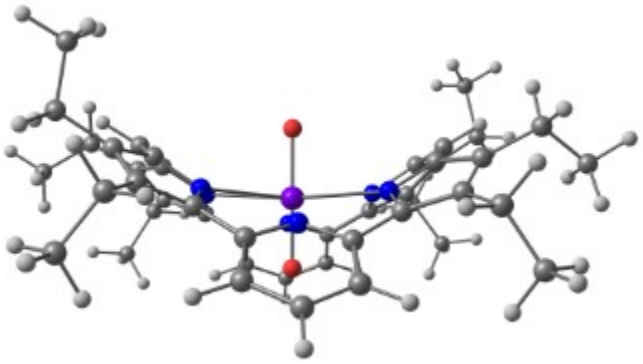 |
| $Cm^{VI}O_2$-$L^-$ | 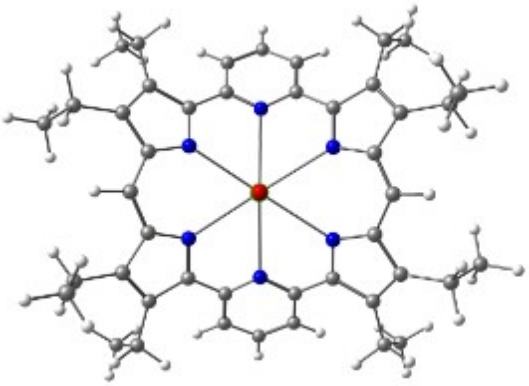 | 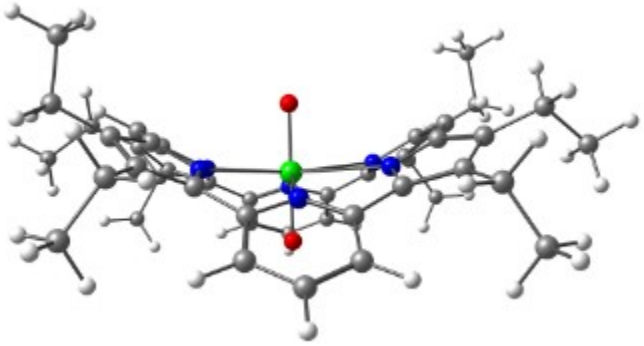 |
| $Bk^{VI}O_2$-$L^-$ | 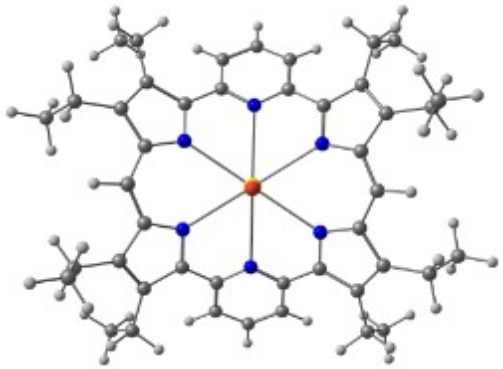 | 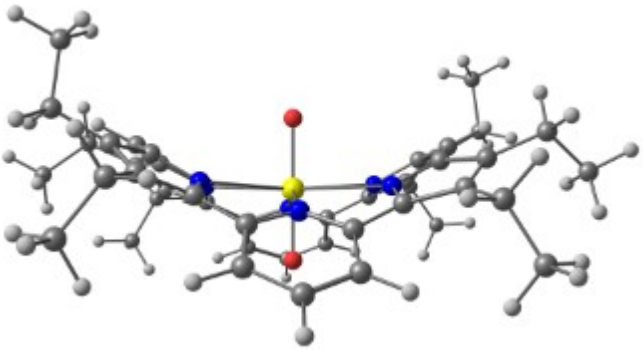 |
| $Cf^{VI}O_2$-$L^-$ | 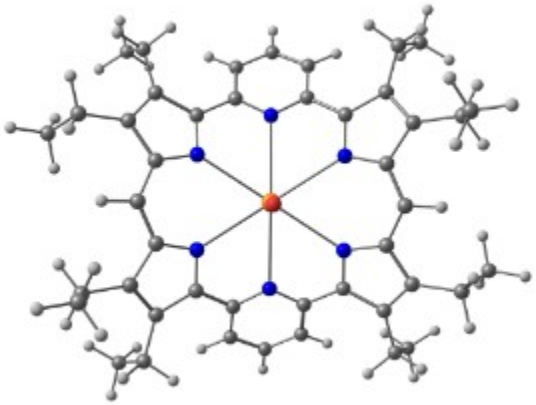 | 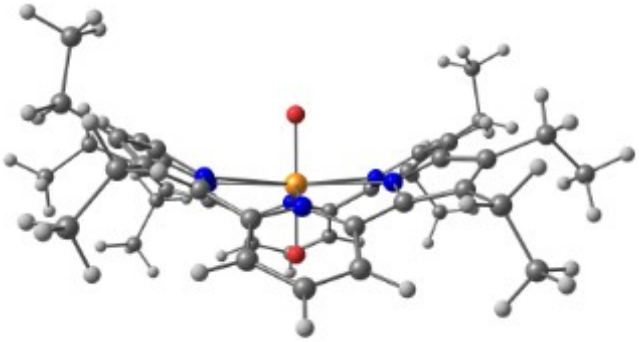 |

**Figure S1. Optimized geometries of Pentavalent and Hexavalent Actinyl - Dipyriamethyrin complexes optimized at PBE/TZP level of theory in gas phase**

| Complex | Top View | Side View |
|---|---|---|
| $AmO_2L^-$ | 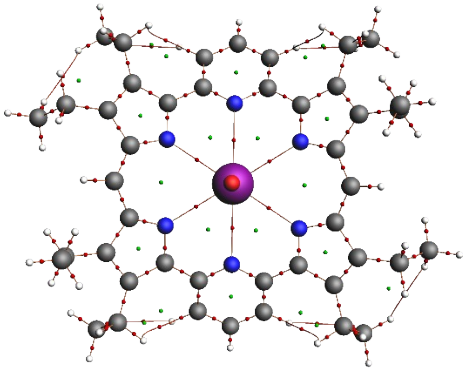 | 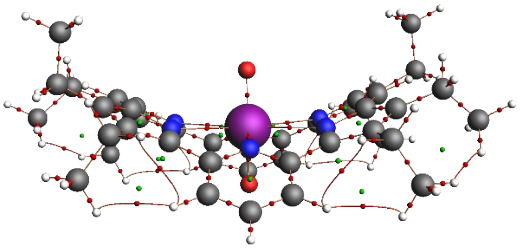 |
| $CmO_2L^-$ | 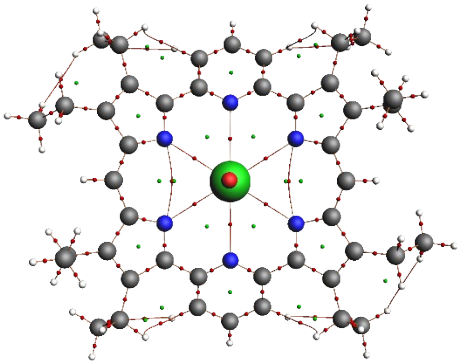 | 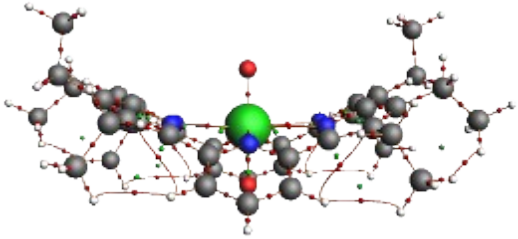 |
| $BkO_2L^-$ | 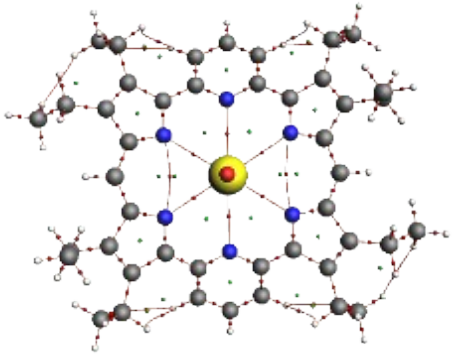 | 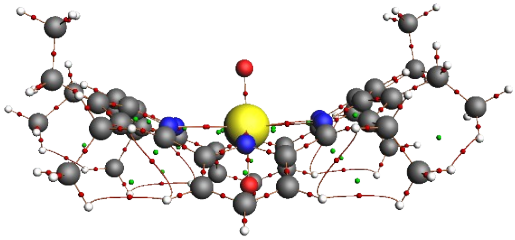 |
| $CfO_2L^-$ | 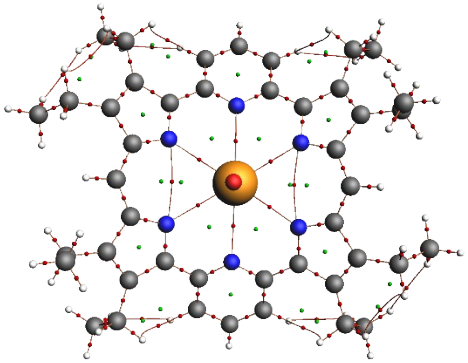 | 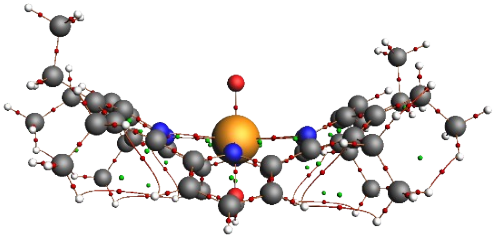 |

| | | |
|---|---|---|
| $AmO_2L$ | 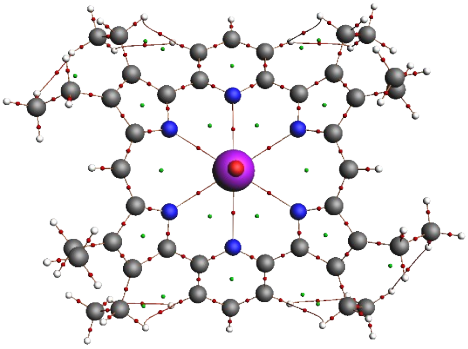 | 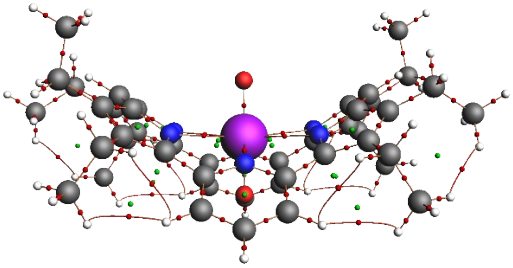 |
| $CmO_2L$ | 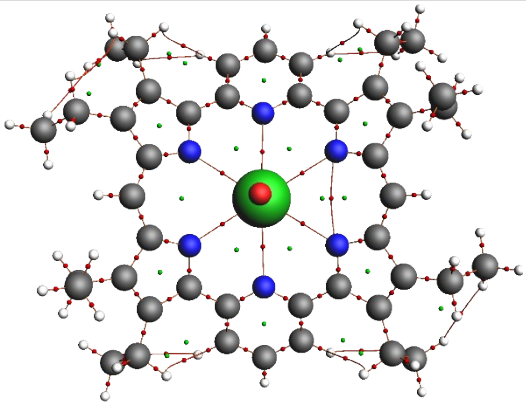 | 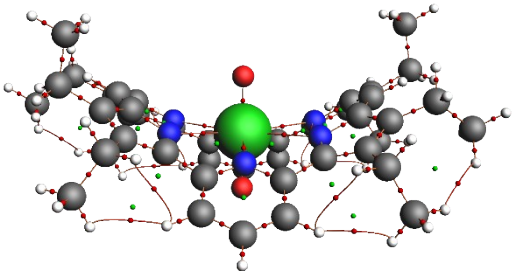 |
| $BkO_2L$ | 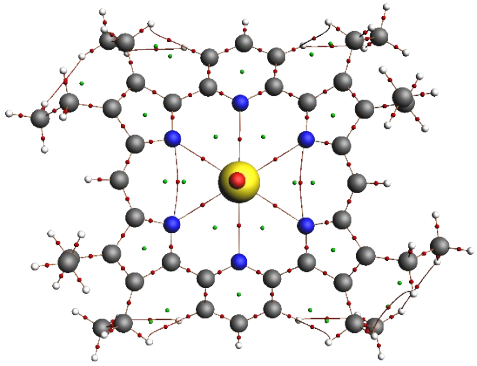 | 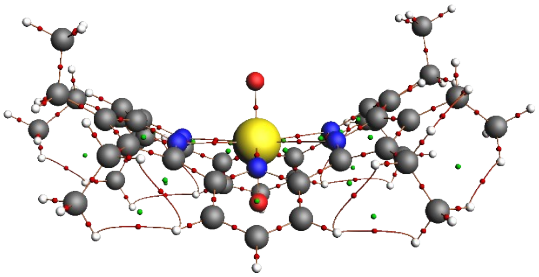 |
| $CfO_2L$ | 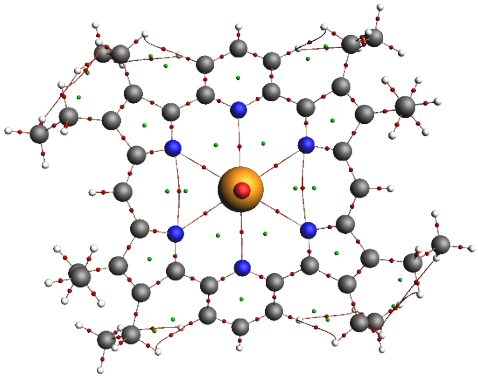 | 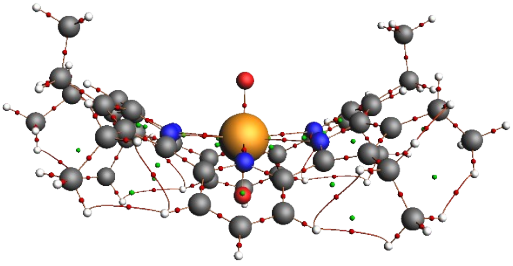 |

**Figure S2. QTAIM molecular topology of $[AnO_2L]^{-1/0}$ complexes, where An=Am, Cm, Bk and Cf where red dots indicate BCP and green dot indicate RCP**

| $[Am^{V}O_2\text{-}Cl_2]^-$ | $[Cm^{V}O_2\text{-}Cl_2]^-$ | $[Bk^{V}O_2\text{-}Cl_2]^-$ | $[Cf^{V}O_2\text{-}Cl_2]^-$ |
|---|---|---|---|
| 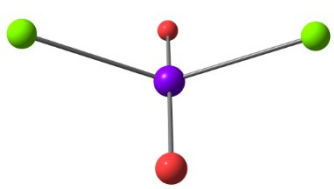 | 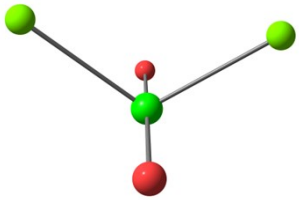 | 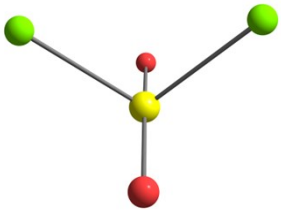 | 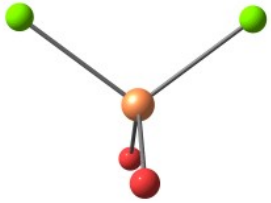 |
| $Am^{VI}O_2\text{-}Cl_2$ | $Cm^{VI}O_2\text{-}Cl_2$ | $Bk^{VI}O_2\text{-}Cl_2$ | $Cf^{VI}O_2\text{-}Cl_2$ |
| 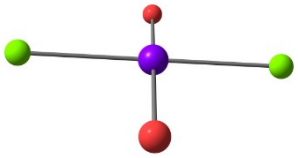 | 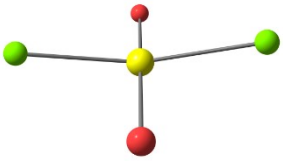 | 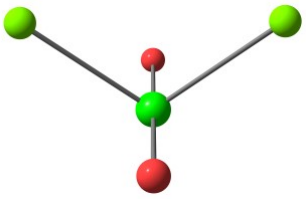 | 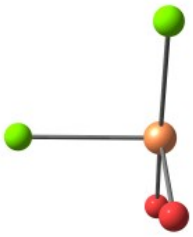 |

**Figure S3. Optimized geometries of $[An^{V}O_2\text{-}Cl_2]^-$ and $An^{VI}O_2\text{-}Cl_2$ in $CH_2Cl_2$ medium.**

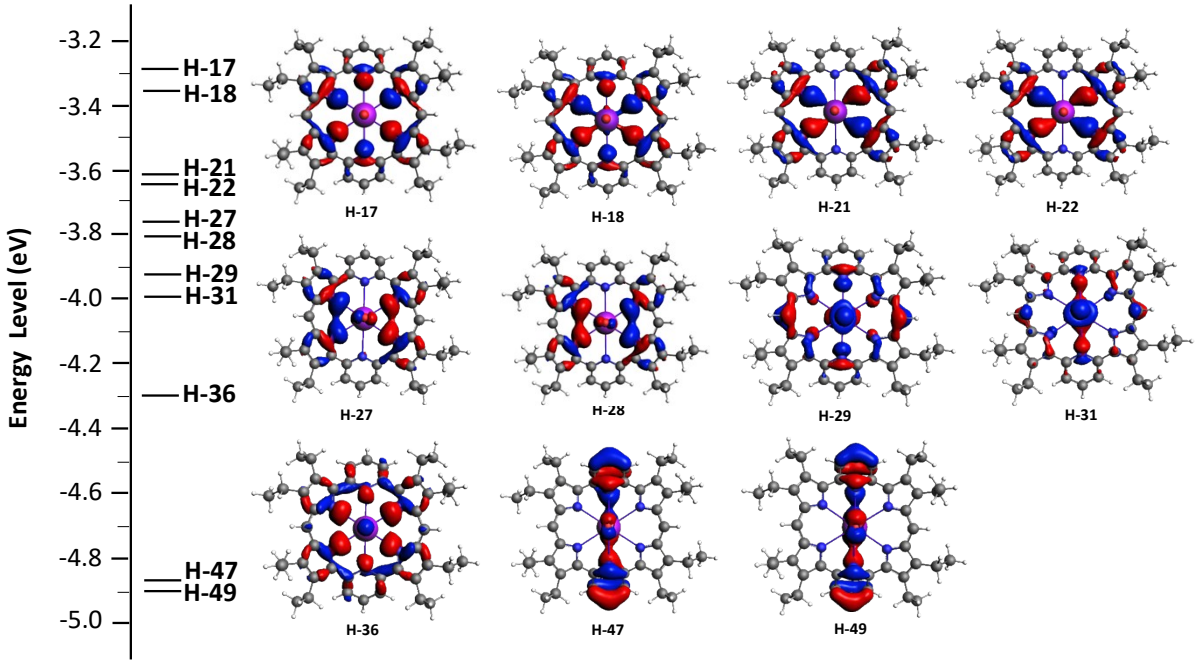


**Figure S4(a). The MOs that represent the stabilizing actinyl-ligand interactions for $Am^{V}O_2$-$L^{-}$ complex (isovalue is 0.03 a.u.). H represents HOMO**

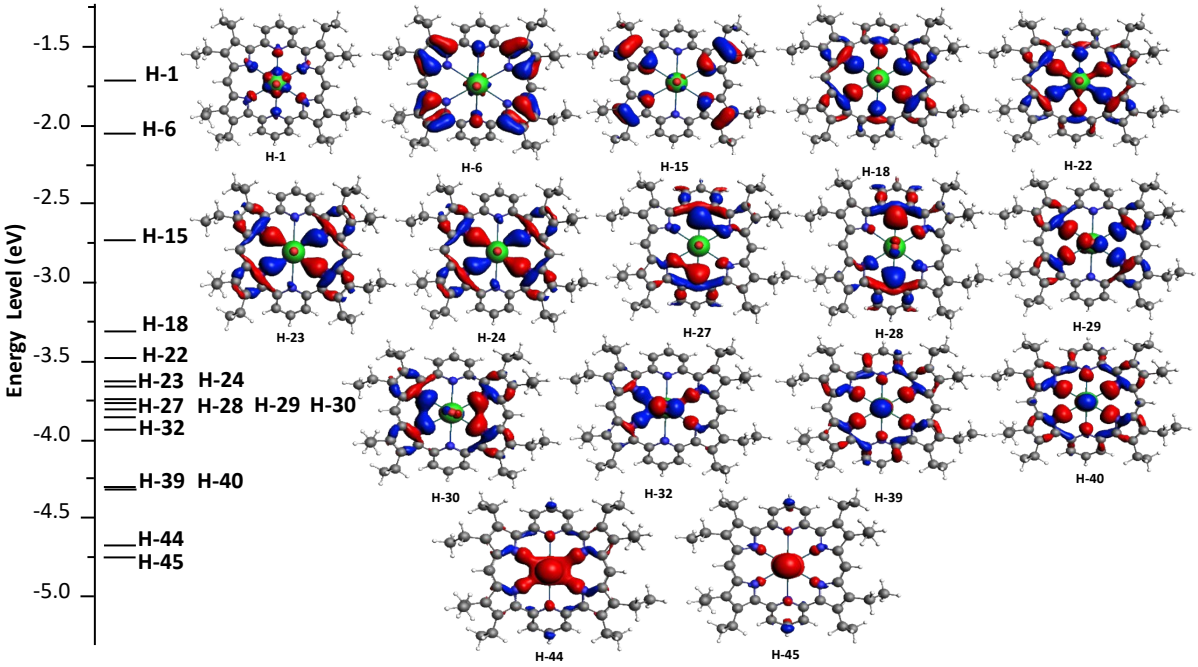


**Figure S4(b). The MOs that represent the stabilizing actinyl-ligand interactions for $Cm^{V}O_2$-$L^{-}$ complex (isovalue is 0.03 a.u.). H represents HOMO**

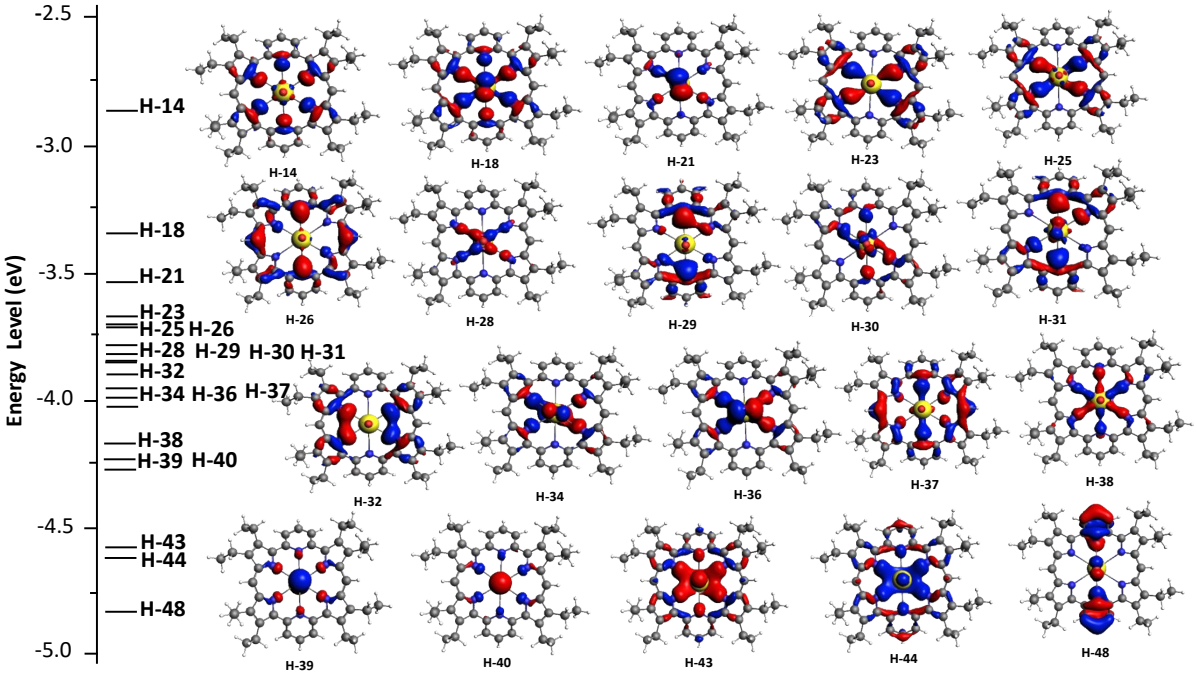


**Figure S4(c). The MOs that represent the stabilizing actinyl-ligand interactions for $Bk^{V}O_2$-$L^{-}$ complex (isovalue is 0.03 a.u.). H represents HOMO**

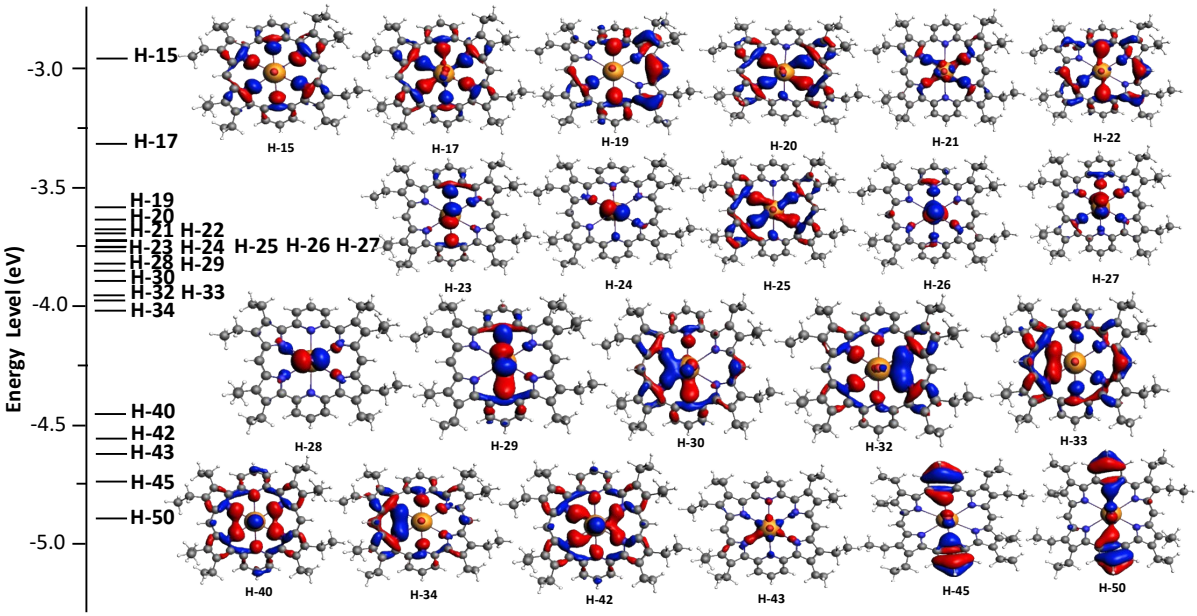


**Figure S4(d). The MOs that represent the stabilizing actinyl-ligand interactions for $Cf^{V}O_2$-$L^{-}$ complex (isovalue is 0.03 a.u.). H represents HOMO**

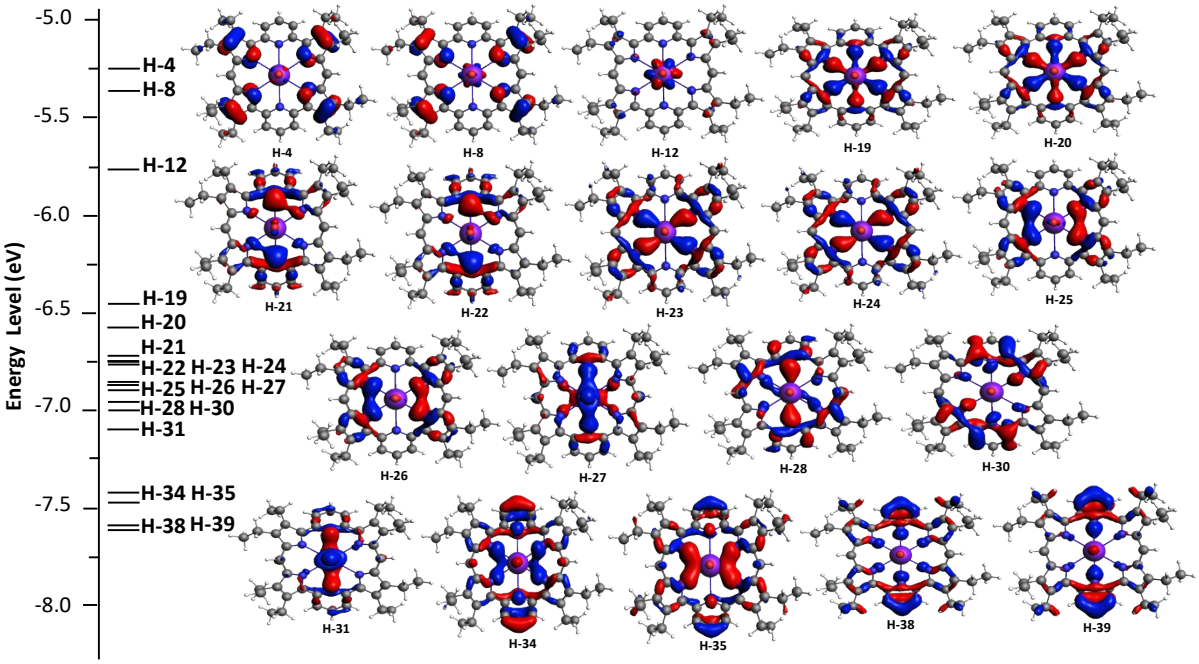


**Figure S4(e). The MOs that represent the stabilizing actinyl-ligand interactions for $Am^{VI}O_2$-L complex (isovalue is 0.03 a.u.). H represents HOMO**

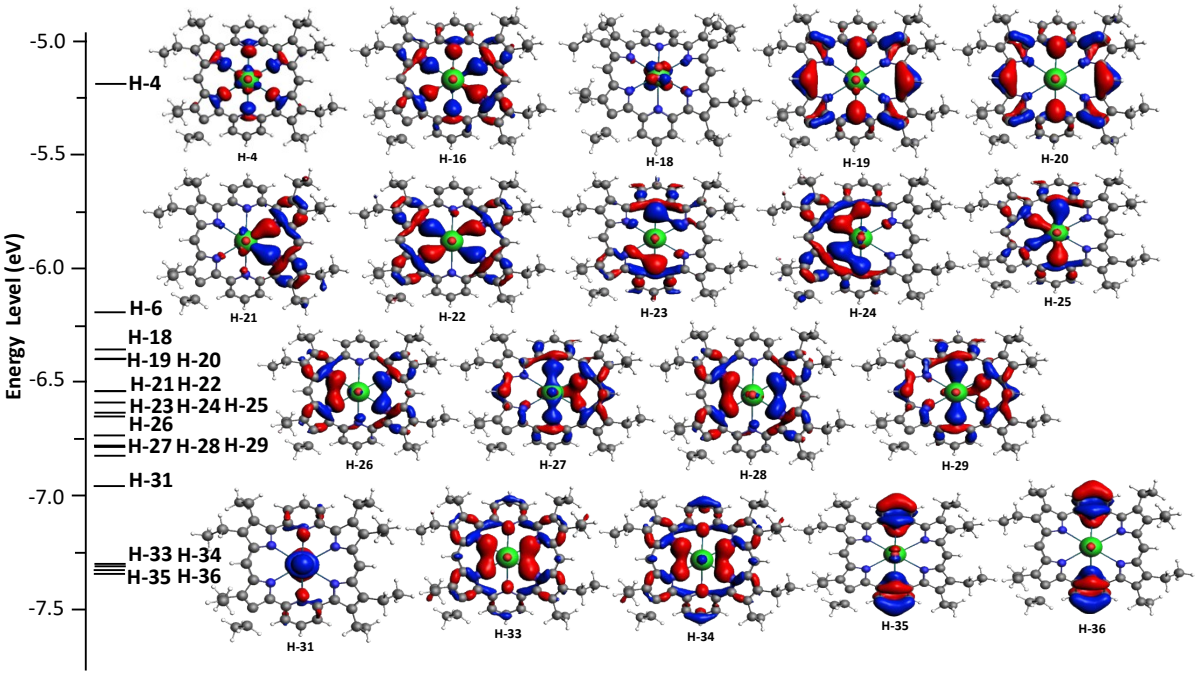


**Figure S4(f). The MOs that represent the stabilizing actinyl-ligand interactions for $Cm^{VI}O_2$-L complex (isovalue is 0.03 a.u.). H represents HOMO**

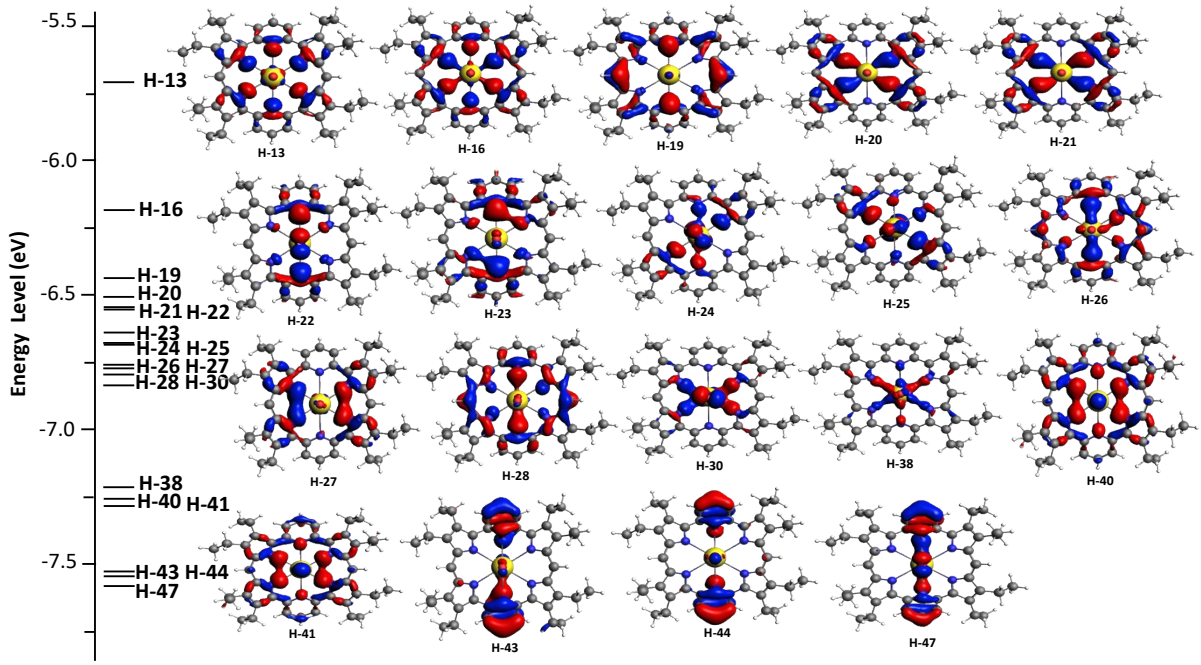


**Figure S4(g). The MOs that represent the stabilizing actinyl-ligand interactions for $Bk^{VI}O_2$-L complex (isovalue is 0.03 a.u.). H represents HOMO**

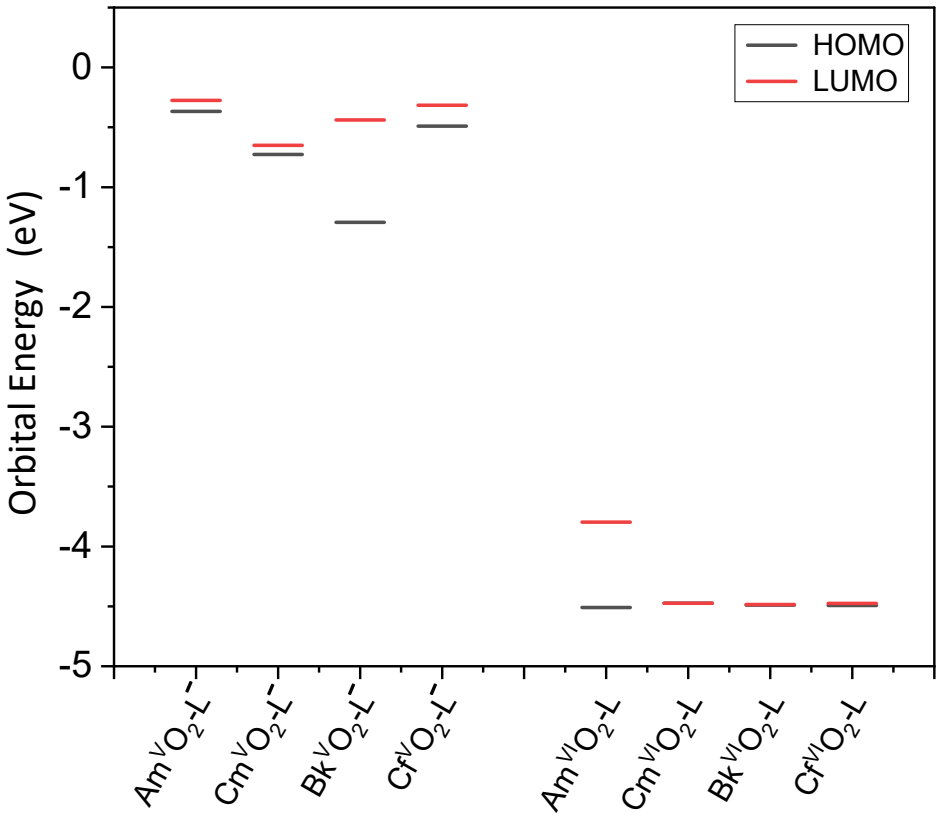


**Figure S5. Molecular orbital energy (eV) observed in the $[An^{V/VI}O_2\text{-}L]^{1-/0}$ complexes**